Design, Synthesis, and 3D QSAR of Novel Potent and Selective Aromatase Inhibitors

Francesco Leonetti,[†] Angelo Favia,[†] Angela Rao,[§] Rosaria Aliano,[†] Anja Paluszcak,[‡] Rolf W. Hartmann,[‡] and Angelo Carotti*,[†]

Dipartimento Farmaco-Chimico, University of Bari, via Orabona 4, I-70125 Bari, Italy, Dipartimento Farmaco-Chimico, University of Messina, viale Annunziata, 98168 Messina, Italy, and Pharmaceutical and Medicinal Chemistry Department, Saarland University, P.O. Box 15 11 50, D-66041 Saarbrücken, Germany

Received June 15, 2004

The design, synthesis, and biological evaluation of a series of new aromatase inhibitors bearing an imidazole or triazole ring linked to a fluorene (A), indenodiazine (B), or coumarin scaffold (C) are reported. Properly substituted coumarin derivatives displayed the highest aromatase inhibitory potency and selectivity over 17-alpha-hydroxylase/17−20 lyase. The modeling of the aromatase inhibition data by Comparative Molecular Field Analysis (CoMFA/GOLPE 3D QSAR approach) led to the development of a PLS model with good fitting and predictive powers (n = 22, ONC = 3, r^2 = 0.949, s = 0.216, and q^2 = 0.715). The relationship between aromatase inhibition and the steric and electrostatic fields generated by the examined azole inhibitors enables a clear understanding of the nature and spatial location of the main interactions modulating the aromatase inhibitory potency.

Introduction

Breast carcinoma is the most common form of female cancer and represents the leading cause of death among women living in industrialized countries.[1,2] In hormone-dependent breast carcinoma, estrogens play a critical role, stimulating cancer cell proliferation.[2,3] Since high serum levels of estrogens favor the progression of breast cancer, two main strategies have been devised by medicinal chemists to control or block the pathological activity of estrogens.[4] The first targeted estrogen receptor activity and yielded the successful development of estrogen receptor antagonists such as Tamoxifen and Raloxifene[5,6] while the second addressed the inhibition of aromatase (AR), a pivotal enzyme involved in the biosynthesis of the estrogen hormones.[7−11] In principle, the stimulation of cancer growth activity by estrogens could be decreased by inhibiting another important enzyme, steroid sulfatase (STS), which provides another source of estrogens, being responsible for the conversion of the inactive stored form (sulfated estrone) to the active form (nonsulfated estrone).[12,13] Finally another enzyme, estrogen sulfotransferase (EST), plays a role in the regulation of the level of circulating estrogens by catalyzing the transformation of active estrogens to inactive estrogen sulfates.[14,15] An overactivation or overexpression of EST could be another winning strategy to halt the progression of hormone-dependent breast cancer. Despite intensive research efforts aimed at the development of biologically active agents targeting STS or EST, no relevant pharmacological results have been published yet.

AR is localized in the endoplasmic reticulum of cells, and it is expressed as a multienzymatic complex consisting of two main components, a form of cytochrome P450 (CYP19) and a NADPH-cytochrome P450 flavoprotein reductase. It catalyzes the conversion of androgens in estrogens through the transformation of the steroid enone A-ring to the aromatic phenolic ring with the concomitant loss of the C_{19} methyl group.

Historically, the first clinically used AR inhibitor has been aminoglutethimide (AG, Chart 1), marketed in the late 1970s.[16] Unfortunately, AG was far from being an ideal drug since it showed several drawbacks, such as high toxicity and lack of selectivity, that have limited its use and induced its ultimate withdrawal. Therefore, the goal of many research groups worldwide has been the development of more potent, selective and less toxic AR inhibitors. This goal has been partly attained with the development of the second generation (i.e. Formestane and Fadrozole)[17] and third generation AR inhibitors, such as Exemestane, Anastrozole, Vorozole, and Letrozole (Chart 1) which are remarkably potent and sufficiently selective drugs.[1]

Third generation AR inhibitors have shown improved efficacy and lower toxicity when compared with the estrogen antagonist Tamoxifen in both the advanced and the early breast cancer. For this reason, the last generation of AR inhibitors, in particular Anastrozole and Letrozole, have been recommended by the FDA as the first line drugs in the therapy of breast carcinoma.[18,19]

Despite these recent undoubted advances, AR inhibitors still present some limitations arising from the possible inhibition of other P450 enzymes, the onset of resistance in the long-term treatment of the breast cancer, and a reduced efficacy in the treatment of the more advanced forms of the tumor.[20,21]

In this context we began a systematic, long term study aiming at the synthesis of new AR inhibitors endowed with better pharmacological and toxicological profiles. In the present report we describe the design and

* Corresponding author. Tel.: ++39−080−5442782; fax: ++39−080−5442230; e-mail: carotti@farmchim.uniba.it.
[†] University of Bari.
[§] University of Messina.
[‡] Saarland University.

10.1021/jm049535j CCC: $27.50
Published on Web 12/07/2004

Chart 1

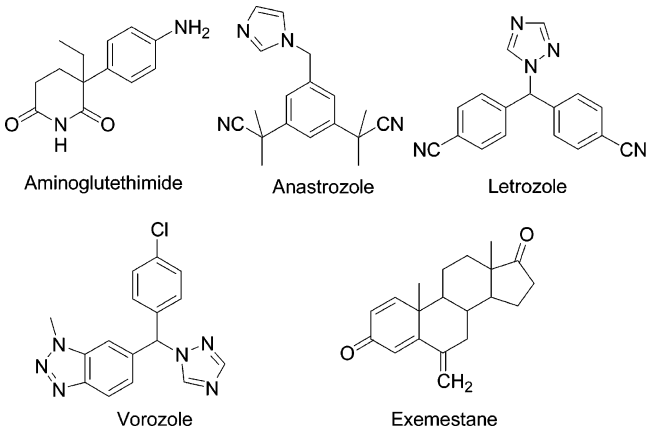

Chart 2

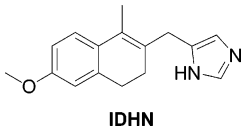

Chart 3

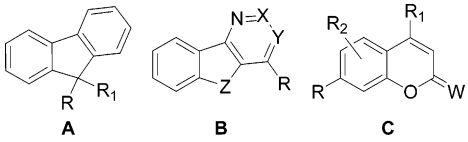

synthesis, and the biological and modeling studies of new AR inhibitors bearing an imidazole or triazole ring linked to a fluorene, indenodiazine, or coumarin scaffolds. Our main aims were the identification of new classes of highly potent AR inhibitors endowed with a good AR (CYP19)/17-alpha-hydroxylase-17−20 lyase (CYP17) selectivity and the development of reliable 3D QSAR models able to detect and locate at the 3D levels the main binding interactions modulating the enzyme affinity and selectivity. It is worth noting that CYP17 is a cytochrome P450 dependent enzyme, involved in the development of prostatic cancer. Huge efforts are currently devoted to the synthesis of CYP17 enzyme inhibitors which may halt the progression of this tumor toward a pharmacologically untreatable advanced form. Recently, Hartmann's group reported the synthesis of some CYP17-selective inhibitors,[22] a representative of which, an imidazolyl-dihydronaphthalene derivative, is reported in Chart 2.

The possibility of preparing molecules acting selectively toward one of these two strictly related enzymes (CYP17 and CYP19) currently represents a very important task for medicinal chemists and may constitute a logical follow up of the present work.[22−24]

The general structure of the azole derivatives designed, synthesized, and tested in the present work are reported in Chart 3. They can be grouped in three types of molecular structures: fluorenes (A), indeno-diazines (-pyrimidines and -pyridazines) (B), and coumarins (C).

Taking advantage of previously developed structure−affinity relationships (SAFIR) for several classes of AR inhibitors, our compounds were designed in order to bear different lipophilic aromatic cores, responsible for extended and strong hydrophobic (or $\pi-\pi$) interactions at the enzyme binding site, and a heterocycle with a nitrogen atom involved in the coordination of the Fe^{2+} of CYP19.[11,25−28]

Table 1. Chemical Structures of Indenodiazine Derivatives **6**, **7**, **10**

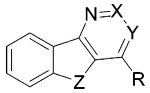

Cpd	Z	X	Y	R
6	CH_2	C-CH_3	N	
7		C-CH_3	N	-
10	CO	N		-

The fluorenyl scaffold **A** was selected because in previous patents an interesting AR inhibitory activity was claimed for a fluorenyl derivative,[29,30] whereas the indenodiazine core **B**, whose synthesis has been exploited in the past by some of us,[31,32] was chosen as a heterocyclic isostere of fluorene. The coumarin scaffold **C** was taken into account because of its structural similarity with chromones, xanthones, and tetralones, three classes of potent AR inhibitors deeply studied by some of us.[33,34]

Coumarins were the most explored class of ligands since some of them, being largely diffused in the plant kingdom, are commercially available or can be easily prepared by simple and consolidated synthetic chemistry. Depending on their substitution pattern, coumarins may display a variety of biochemical and pharmacological activities, generally associated to a low toxicity.[35−38] Known structure−activity relationships of coumarins have been therefore properly taken into account in the molecular design phase in order to avoid the appearance of additional, unwanted biological effects.[39−41] Appropriate azole substituents were then introduced on the coumarin ring to obtain a set of molecules with a high degree of molecular diversity and hence particularly useful for the derivation of sound structure-affinity relationships.

Chemistry. Indenodiazine derivatives **6**, **7**, and **10** (Table 1) were synthesized according to already published methods.[31,32]

As shown in Scheme 1, the reaction of **4** with *N*-bromosuccinimide (NBS) in CCl_4 in the presence of a catalytic amount of 2,2′-azobisisobutyronitrile (AIBN) gave the bromo derivative **5** that was reacted with imidazole in dioxane to afford the expected product **7** along with derivative **6**, likely arising from **7** through an allylic transposition.

Bromination of the 3-methyl-5*H*-indeno[1,2-*c*]pyridazine derivative **8** with NBS and AIBN gave the bromomethyl derivative **9** that upon treatment with imidazole in dioxane afforded **10** (Scheme 2).

The fluorenyl derivatives **13**−**17** (Table 2) were prepared from the commercially available 9-bromo-9*H*-fluorene (**11**) and 9-bromo-9-phenyl-9*H*-fluorene (**12**), respectively, by standard SN type reaction with the corresponding azoles.

Compounds **13** and **14** have been already described in two different patents, but only **13** has been tested as aromatase inhibitor.[29,30] For the triazole derivatives

Scheme 1. Synthesis of Indeno[1,2-*d*]pyrimidines **6** and **7**[a]

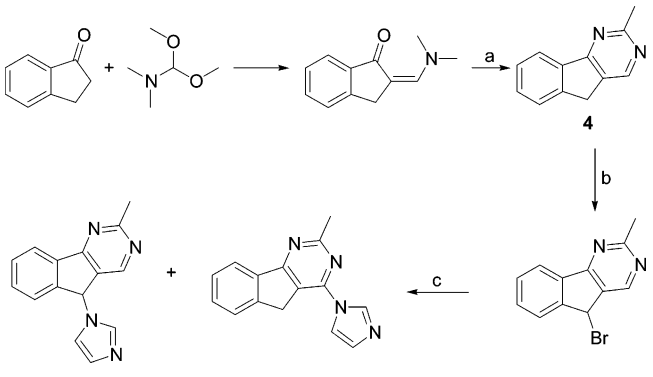

[a] (a) Acetamidine, MeONa, EtOH; (b) NBS, AIBN, CCl_4; (c) imidazole, dioxane.

Scheme 2. Synthesis of Indeno[1,2-*c*]pyridazine Derivative **10**[a]

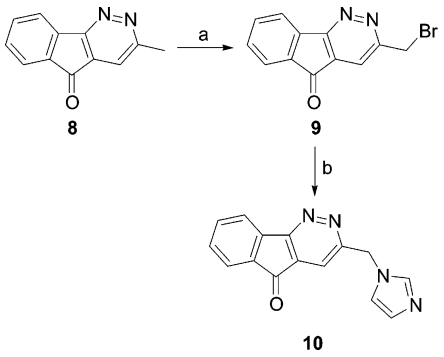

[a] (a) NBS, AIBN, CCl_4; (b) imidazole, dioxane.

Table 2. Synthesis and Chemical Structures of Fluorenyl Derivatives **13**–**17**

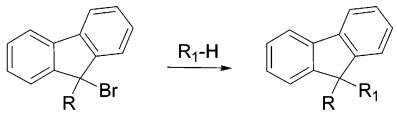

11, R = H; **12**, R = Ph — **13-17**

Cpd	R	R_1
13	H	
14		
15		
16		
17		

15–**17**, the synthesis was carried out using NaH as the base in anhydrous DMF at 90 °C, while imidazole derivatives **13** and **14** were prepared in refluxing dioxane.

The most represented class of compounds reported in this paper are the coumarins (compounds **18**–**35** in Table 3). The straightforward preparation of compounds **24**–**28** and **30**–**33** followed a common synthetic scheme, characterized by an initial NBS-AIBN (or benzoyl peroxide) bromination of the appropriate methylcoumarin in CCl_4 followed by an SN reaction with imidazole

Table 3. Chemical Structure of Coumarin Derivatives **18**–**35**

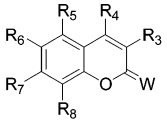

18-**34**, X = O; **35**, W = S

Cpd	R_3	R_4	R_5	R_6	R_7	R_8
18		H	H	H	OCH_3	H
19	H		H	H	H	H
20	H		H	H	OCH_3	H
21	H		H	H	OCH_3	H
22	H		H	H	H	H
23	H		H	H	OCH_3	H
24	H		H	H		H
25	H	H		H	OCH_3	H
26	H	H	H		H	H
27	H	H	H	H		H
28	H	H	H	H		H
29	H	H	H	H		H
30	H	H	H	H	OCH_3	
31			H	H	H	H
32			H	H	OCH_3	H
33	H		H	H	OCH_3	H
34	H		H	H		H
35	H	H	H		H	H

or 1,2,4 (or 1,2,3)-triazole, generally in refluxing THF and K_2CO_3. Compounds **22**, **23**, and **29**, bearing a longer bridge between the coumarin and the imidazole rings, were synthesized from suitable hydroxycoumarins through two consecutive SN reactions, first with 1,2-dibromoethane and then with imidazole.

Some starting coumarins used for the preparation of compounds **18**–**35** were synthesized following the classical von Pechmann's procedure,[42,43] from resorcinol (or its monophenyl ether as in the synthesis of **24**) and a suitable β-ketoester under strong acid catalysis (H_2SO_4 or H_2SO_4/CF_3COOH). Compounds **22**, **23**, **26**, **29**, and **31** were prepared from the commercially available 4-hydroxycoumarin, 4-hydroxy-7-methoxycoumarin, 6-methylcoumarin, 7-hydroxycoumarin, and 4-methyl-3-phenylcoumarin, respectively. The synthesis of compounds **20** and **21** was carried out by reacting the commercially available 4-bromomethyl-7-methoxycoumarin with imidazole or 1,2,4-triazole, respectively, in refluxing THF using K_2CO_3 as the base and tetrabutylammonium iodide (TBAI) as the catalyst. Compound **18** was synthesized through methyl bromination and a successive SN reaction with imidazole, from 7-methoxy-3-methylcoumarin, obtained in turn through a cyclization reaction of 2,4-dihydroxybenzaldehyde with propionic anhydride, sodium propionate, and piperidine, followed by an alkylation with CH_3I and NaH in DMF. 4-Chloromethylcoumarin, prepared according to the classical von

Pechmann's procedure from phenol and ethyl 4-chloro-3-oxobutanoate, was reacted with imidazole, K_2CO_3, and TBAI in refluxing THF to yield **19**. The same synthetic protocol was used for the preparation of **34** from 4-chloromethyl-7-hydroxycoumarin, prepared in turn as the 4-chloromethylcoumarin, substituting phenol with resorcinol. Finally, treatment of coumarin **26** with Lawesson's reagent gave the thiocoumarin derivative **35**.[44]

Biological Assays. The molecules reported in this paper were tested for their inhibitory activities against AR (CYP 19) and 17α-hydroxylase/C17,20-lyase (CYP17), two related P450 enzymes, which are responsible for catalyzing the final step in estrogen and androgen biosynthesis, respectively. In the case of CYP19, human placental microsomes were used as source of the enzyme and [1β,2β-^{3}H] testosterone or [1β-^{3}H] androstenedione as substrates as described by Thompson and Siiteri,[45] using our modifications,[46,47] In the case of highly potent compounds, the IC_{50} values were determined. For determination of CYP17 inhibition, human testicular microsomes[48] or microsomes from *E. coli*-expressing human CYP17[47] and progesterone as substrate were applied; the inhibition data are shown in Table 4 as percent of inhibition at the indicated concentrations.

Results and Discussion

The first analysis of the structure−affinity relationship concerned a general comparison of the enzyme affinities among the three classes of compounds described in this report. Indenodiazines gave the poorest biological results whereas coumarins represented the most interesting class of inhibitors since both their potency and CYP19/CYP17 selectivity are considerably high. Fluorenyl derivatives also displayed a high inhibitory potency against AR along with a significant degree of selectivity but their synthetic accessibility is not as convenient as for coumarins and therefore structural modifications aimed at improving potency and optimizing ADMET properties (absorption, distribution, metabolism, excretion, and toxicity) would be difficult and more time-consuming.

The analysis of SAFIR carried out separately on the three classes of compounds led to the following main considerations.

The low inhibitory potency of the indeno[1,2-*d*]pyrimidine **7** indicates that the substitution of a benzene with a pyrimidinyl ring has no positive effect on binding (compare **7** vs **13**). However, a significant degree of CYP19/CYP17 selectivity would be expected taking into account that no inhibition of the CYP17 was observed at the highest tested concentration of inhibitor (125 μM). Much worse affinity and selectivity data have been obtained for the indeno[1,2-*c*]pyridazine **10**, suggesting that this heterocyclic scaffold is unsuitable for the development of potent and selective AR inhibitors**.**

It is worth noting that the inhibitory activity of compounds **7** and **10**, albeit low, has to be related to the iron-coordinating properties of the nitrogen of the imidazole moiety, since the nitrogen atoms of their diazine rings should not possess such a capability. In fact, in the case of **7**, the presence of a methyl group between the two pyrimidine nitrogen atoms likely impedes the coordination of the iron ion, and a similar consideration applies to ligand **10** where the lone pair of neither of the two vicinal nitrogen atoms of the pyridazine moiety is available for an efficient metal coordination due to both steric and electronic reasons.

Table 4. Observed (CYP19[a] and CYP17[b]) and Calculated (CYP19) Inhibitory Activities of the Indicated Compounds

compd	CYP17[c]	CYP19[d]	pIC_{50} (obs)[e]	pIC_{50} (calc)[f]	residuals[g]
7	0%	2.85	5.55	5.50	0.05
10	64%	26.63	4.57	4.63	−0.06
13	nd	2.85	5.55	5.70	−0.15
14	9%	0.074	7.13	6.64	0.49
15	7%	44%	[h]	-	-
16	2%	30%	[h]	-	-
17	6%	4.00	5.40	5.83	−0.43
18	43%	2.82	5.55	5.74	−0.19
19	1%	2.10	5.68	5.76	−0.08
20	14%	0.280	6.55	6.36	0.19
21	4%	3.60	5.44	5.33	0.11
22	2%	0.76	6.12	6.47	−0.35
23	nd	12%	4.00	3.80	0.20
24	26%	0.051	7.29	7.22	0.07
25	15%	0.168	6.77	6.55	0.22
26	0%	0.144	6.84	6.71	0.13
27	8%	0.680	6.17	5.96	0.21
28	2%	60%	4.50	4.75	−0.25
29	14%	60%	4.50	4.51	−0.01
30	9%	59%	4.50	4.25	0.25
31	9%	5.13	5.29	5.29	0.00
32	0%	0.106	6.97	6.85	0.12
33	20%	27%	[h]	-	-
34	3%	0.150	6.82	6.99	−0.17
35	8%	1.13	5.95	6.50	−0.55
IDHN[i]	0.110	17.0	[h]	-	-

[a] Human placental microsomes. Testosterone (2.5 μM) was used as substrates and aminoglutethimide (AG) as reference (IC_{50} values 18.5 μM), except for compounds **23**, **30**, and **33** for which androstendione (0.5 μM) was used. [b] Human testicular microsomes or microsomes from *E. coli*-expressing human CYP17 (identical inhibition values were obtained using different enzyme sources). Concentration of substrate (progesterone): 25μM; concentration of inhibitor: 2.5 μM, except for **7** (125 μM) and for **26**, **31**, and **32** (0.5 μM). [c] Data expressed as percent of inhibition at the concentration indicated in note *b*, except for IDHN whose affinity is expressed as IC_{50}; nd, not determined. [d] Data are expressed as IC_{50} (μM) or percent of inhibition at 36 μM. For **16** and **17** and **28** and **29**, the indicated percent refer to a 25 μM concentration. [e] Data expressed as pIC_{50} (CYP19), used for the derivation of PLS model ES (Table 5). [f] Calculated pIC_{50} from PLS model ES (Table 5). [g] pIC_{50}(obs) − pIC_{50}(calc). [h] Not included in the derivation of CoMFA models (see text). [i] This compound (see Chart 2), with an inverted CYP17/CYP19 selectivity, has been added as a reference for comparison.

A final consideration suggesting no further development of these classes of compounds concerns their synthesis that requires a demanding multistep synthetic protocol and, moreover, leads, sometimes, to racemic mixtures which would require further efforts for the separation of enantiomers.

Fluorenyl derivatives **13**−**17** represent a more interesting class of AR inhibitors. The most active compound is derivative **14** with an IC_{50} = 74 nM and a good CYP19/CYP17 selectivity. The SAFIR of these products indicated that the imidazolyl derivatives **14** is more active than the corresponding triazolyl derivatives **15**−**17**. As already reported in the literature, the capability of the nitrogen to coordinate the iron of the heme is reduced by the presence of a vicinal nitrogen for electronic (lower availability of the lone pair) and/or steric effects (reduced accessibility to the iron). The above considerations led to the following rank order of

activity: **14** ≫ **15** > **17** > **16**. Furthermore, the introduction of an additional lipophilic group (i.e. the 9-phenyl substituent) improves the inhibitory activity, as can be seen in the comparison of the IC_{50}s of **14** (74 nM) and **13** (2850 nM). The high activity displayed by **14** is particularly interesting because this derivative does not show in the fluorenyl ring any hydrogen bonding group, a structural feature observed in many potent AR inhibitors reported in the literature.[28] Therefore, the good inhibitory activity of **14** is principally determined by highly favorable hydrophobic interactions experienced by both the fluorenyl scaffold and the 9-phenyl ring.

As outlined above, coumarins present the most interesting biological activities. The compound of this series with the highest AR affinity is the phenoxy derivative **24** with an IC_{50} of 51 nM (363-fold more active than AG) and a good degree of CYP19/CYP17 selectivity. The most salient features emerging from the SAFIR of coumarin derivatives **18**−**35** can be summarized as follows:

(a) The position of the 1-methylimidazolyl substituent on the coumarin ring plays a central role in the modulation of the inhibitory activity. The effects observed in the series of unsubstituted derivatives do not parallel those observed in the corresponding series of 7-methoxy-substituted congeners. Indeed, the rank of affinity for the unsubstituted and methoxy-substituted series, respectively, was as follows (the position of the 1-methylimidazolyl substituent is indicated in parentheses): **26** (6)> **27** (7)> **19** (4), and **25** (5) ≥ **20** (4)> **18** (3) > **30** (8).

These results are not so surprising since the methoxy substituent, according to a recently proposed pharmacophore hypothesis,[26] may act as hydrogen bond acceptor depending on its spatial position relative to the nitrogen atom coordinating the iron ion. In other words, as we will discuss later, for the methoxy-substituted derivatives a variety of binding modes are possible which may even differ from the binding modes of the corresponding unsubstituted coumarin derivatives.

(b) The length of the bridge linking the imidazole to the coumarin ring was another important structural element modulating the enzyme affinity. The biological results indicate an opposite effect of the bridge length in 4- and 7-substituted derivatives, as can be seen comparing the affinity of **19** with **22** (2100 vs 760 nM) and **27** with **29** (680 vs nearly 20000 nM).

(c) The introduction of a methoxy group at the 7-position of the coumarin ring determines an opposite effect on the affinity of derivatives **19** and **22**. In fact, while in the former the activity increases (280 vs 2100 nM, in **20**), in the latter it strongly decreases (from 760 to ≫ 36000 nM, in **23**). Most likely, the methoxy derivatives **20** and **23** bind in different enzyme regions, being characterized by a quite different distance between the imidazolyl and the coumarin rings. As a result, the 7-methoxy group might engage in different interactions at the enzyme binding site, favorable for **20**, likely a hydrogen bond, and unfavorable for **23**, likely a steric repulsion. This hypothesis was fully confirmed by our subsequent CoMFA/GOLPE study.

(d) The effect on the affinity obtained by introducing a phenyl substituent in the coumarin scaffold is position-dependent. In fact, 3-phenyl derivative **31** shows an affinity lower than the 3-unsubstituted congener **19** (5100 vs 2100 nM), while the 4-phenyl-substituted derivative **32** has an inhibitory activity much greater than the 4-unsubstituted congener **18** (110 vs 2820 nM).

(e) The substitution of the imidazolyl with a pyridyl ring did not lead to any positive result. In fact, 4-(4-pyridyl) derivative **33** shows a very low inhibitory potency. Most likely, the structural rigidity of **33** and the unique and fixed direction of the nitrogen lone pair of the 4-pyridyl substituent might not allow a correct orientation of the ligand for an efficient coordination of the iron atom, differently from the 1-methyl(alkyl)-imidazolyl derivatives which are more flexible.

(f) The carbonyl group of the coumarin lactone ring seems an important structural determinant for the activity since the thiocarbonyl derivative **35** is significantly less active than **26** (140 vs 710 nM).

(g) A favorable interaction at the 7-position of the coumarin rings may be hypothesized by comparing the activity of the parent 4-(1-methylimidazolyl) derivative **19**, with those of the 7-methoxy (**20**), 7-phenoxy (**24**), and 7-benzyloxy (**34**) congeners. The following rank of activity was observed: **24** > **34** > **20** ≫ **19**. This affinity enhancement may be ascribed to two favorable interactions, the formation of an hydrogen bond by the 7-oxygen atom (i.e. **20** ≫ **19**) and a lipophilic or $\pi-\pi$ stacking interaction of the phenoxy or benzyloxy group (**24** > **34** > **20**).

(h) A single CH_2 seems to be an optimal bridge to link the imidazolyl to the coumarin ring; its replacement with the longer OCH_2CH_2 spacer reduces the biological activity (**20** ≫ **23**; **27** ≫ **29**), with only the exception of **22**, which is more potent than **19**.

Most of the above observations were substantiated in the subsequent CoMFA study.

Regarding the CYP17 inhibition data, it is striking that most compounds showed either no significant or only marginal inhibition of this P450 enzyme. The only exception were compounds **10** and **18** exhibiting 64 and 43% inhibition at a concentration of 2.5 μM. Thus, they were similarly active as the reference ketoconazole, a nonselective CYP inhibitor, which under the same experimental conditions exhibited a IC_{50} value of 4.5 μM. Taking into consideration that CYP17 inhibitors, exhibiting IC_{50} values in the low nanomolar range, have been developed,[22] it can be concluded that the fluorene, indenodiazine, and coumarin polycyclic systems are not appropriate scaffolds for the design of potent CYP17 inhibitors. More important, the observed lack of CYP17 inhibition leads to a very high degree of CYP19/CYP17 selectivity, which is not only important for the design of more selective CYP19 inhibitors but also for the modeling of the aromatase inhibition data as it is described in the following 3D QSAR study.

A CoMFA study, limited to the AR inhibition data, was performed on 22 out of 25 nonsteroidal AR inhibitors of this work. The excluded molecules, all characterized by a very low AR affinity, were **33**, which was structurally quite different from all the other compounds, and **15** and **16** which might bind differently to the enzyme since the vicinity of two nitrogen atoms in both the 1,3,4- and 1,2,3-triazole rings may preclude the coordination of the nitrogen lone pair to the porphyrinic iron, a common feature of the binding mode of all the other inhibitors. Most of the compounds considered in

Table 5. Statistical Figures of CoMFA PLS Model

model	field	n^a	ONC[b]	r^{2c}	sd[d]	r^2_{cv}[e]	sd_{cv}[f]
S	ste	22	3	0.914	0.280	0.562	0.632
E	ele	22	3	0.932	0.248	0.688	0.533
ES	ste + ele	22	3	0.949	0.217	0.715	0.510

[a] Number of inhibitors considered. [b] Number of optimal PLS components. [c] Squared correlation coefficient. [d] Standard deviation of error of calculation. [e] Leave-one-out squared cross-validated correlation coefficient. [f] Standard deviation of error of predictions.

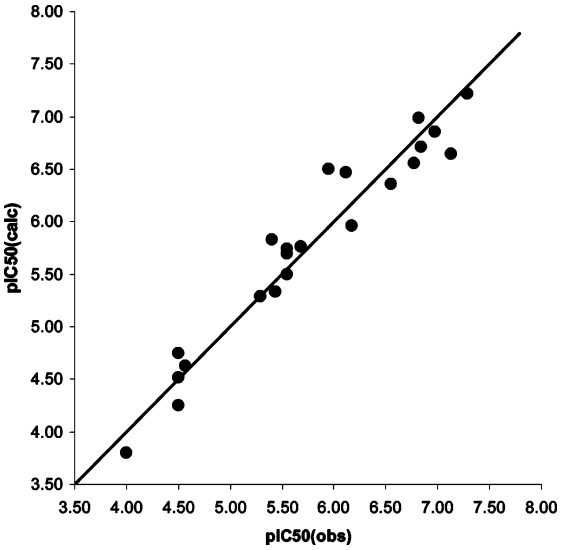

Figure 1. Plot of calculated versus observed pIC_{50} from PLS model ES (Table 5).

the present study (17 compounds) shared two common molecular fragments, a coumarin ring and an azole ring with a nitrogen atom able to coordinate the Fe^{2+} of the AR porphyrin ring. Three fluorenyl (**13**, **14**, and **17**) and two indenodiazine (**7** and **10**) derivatives were also taken into account in our 3D QSAR study. The AR inhibition data of the examined compounds are reported as pIC_{50} in the fourth column of Table 4.

For the derivation of 3D QSAR models, PLS analyses were performed adopting the 'leave-one-out' cross-validation procedure. Steric and electrostatic potentials, calculated on a GRID box around the aligned molecules by using a positively charged sp^3 carbon atom as a probe, were analyzed according to the CoMFA/GOLPE approach (see Experimental Section for further details).

The statistical figures of the PLS analyses, listed in Table 5, showed that the one-field electrostatic model (E) presented slightly better statistics than the corresponding steric one (S). The combination of the two CoMFA fields gave a PLS model with improved statistical figures and a balanced field contributions (37% Ele, 63% ste) in the ES model in Table 5.

The good fitting power of PLS model ES can be easily appreciated both from the analysis of the residuals in Table 4 and of the plot of the observed versus predicted values reported in Figure 1. Only three inhibitors, i.e., **14**, **17**, and **35**, were poorly predicted (residuals ≥ 2 sd). While for the imidazolyl fluorenyl derivative **14** no easy explanation can be found, the poor predictions for the other two inhibitors might be ascribed to their poorly represented structural features in the data set. Indeed, besides **17**, only two more 1,2,4-triazolyl derivatives (i.e. **21** and **22**) are present in the data set and, even worse, **35** is the only thiocoumarin examined.

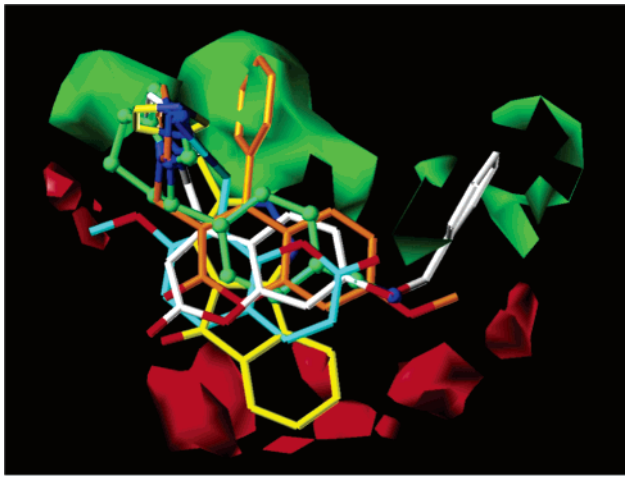

Figure 2. Steric isocontour maps from PLS model ES (contour levels: 0.0005 green, −0.00043 red). Highly (**32** and **34**, orange and white bonds, respectively) and low active (**10** and **30**, yellow and cyan bonds, respectively) compounds are shown, along with *S*-fadrozole (ball-and-stick green model), to help interpretation.

Figure 3. Electrostatic isocontour maps from PLS model ES (contour levels: 0.0013 cyan, −0.0009 magenta). The highly (**24** and **26**, white and orange bonds, respectively) and low (**28**, yellow bonds) active compounds are shown, along with *S*-fadrozole (ball-and-stick green model), to help interpretation.

The results of the CoMFA/GOLPE analysis can be more efficiently represented graphically as coefficient isocontour maps (stdev X coeff) as shown in Figures 2 and 3. In this way, it is possible to detect and locate easily, at the 3D level, the key steric and electrostatic interactions modulating the AR inhibitory potency.

Different color codes were used to contour regions where the main interactions take place. Green color contour regions where the addition of steric bulk increases the activity, whereas a decrease of activity was observed when molecular moieties occupy the zones represented in red. The cyan electrostatic contours indicate zones where the increase of electron density is detrimental for the inhibitory activity, whereas in the regions contoured in magenta an increase of negative charge enhances the affinity. *S*-Fadrozole was added to both figures to help a qualitative comparison with previously developed CoMFA models.[26,27]

The analysis of the main statistical signals represented in the steric and electrostatic contour maps of Figures 2 and 3 unveils that a high inhibitory potency is associated to molecules placing aromatic (lipophilic) rings in two green regions, top right (i.e. **34**), and central part (i.e. **32**) of Figure 2 and electronegative atoms (oxygen atoms) in a putative magenta region, bottom right in Figure 3. The latter is also reached by the nitrogen of the key *p*-cyano substituent of *S*-fadrozole.

Low active inhibitors are experiencing negative steric contacts in a series of fragmented red regions located in the bottom part of Figure 2 (i.e. **10**) and in another red zone visible in the left central part of the same figure (i.e. **30**, with its OCH_3 substituent). Another significant electrostatic signal, justifying, at least in part, the lower activity of 1,2,4-triazole compared to the imidazole derivatives, can be seen on the left corner of Figure 3 where a cyan zone, indicating unfavorable interactions for highly electronegative atoms, is definitely contacted by the N2 nitrogen atom of triazoles (i.e. **28**).

The main structural features influencing the inhibitory potency, clearly detected in the CoMFA maps, are in good agreement with the most salient observations made previously in the SAFIR analysis.

Conclusion

In summary, a number of new coumarin and fluorene imidazolyl derivatives described in this paper proved to be remarkably potent and selective AR inhibitors. In comparison with already reported AR inhibitors of similar potency, coumarin derivatives present several advantages, such as a facile and straightforward synthesis, and expectedly favorable ADME properties and toxicological profile as the coumarin scaffold is present in many natural and dietary products,[37] as well as in some drugs.[41] However, some coumarin derivatives may constitute a good substrate/inhibitor for some P450 metabolic enzymes.[49,50] The SAR recently emerged also at this level[51] may help the design of new compounds with the desired P450 selectivity and ADMET properties. Simple coumarin chemistry may facilitate the attainment of such important goals since it may allow the introduction of a variety of properly chosen substituents all around the coumarin ring. Thus, an easy variation of the local and global physicochemical properties of the selected molecules may be possible.

Among the tested inhibitors, the two coumarin derivatives **24** and **34** can be considered promising leads for further structural modifications guided by the valuable information derivable from our detailed analysis of the SAFIR and from the close examination of the isocontour maps developed from the very informative and statistically significant two-field PLS model ES. Another class of compounds that may deserve a particular attention for further advancements are the fluorenyl derivatives. As for coumarins, the synthesis of suitably functionalized fluorenyl derivatives is not very difficult, and proper substituents may be inserted on the two benzo moieties and on the 9-phenyl substituent to optimize the pharmacodynamic and pharmacokinetic properties of this class of inhibitors. However, differently from coumarins, the introduction of a substituent on one benzo moiety would afford racemic mixtures, whose enantiomeric resolution would indeed require further efforts, but will lead to chiral compounds which may be particularly useful to study in full detail enantioselective interactions at the enzyme binding sites.

As a final remark, it is worth considering that our CoMFA-GOLPE model ES, being based on a relatively low number of inhibitors, needs to be enlarged and improved. Nonetheless, along with previously developed CoMFA models[26,27] that are in agreement, model ES may help guide the synthesis of novel different classes of ligands aiming at the refinement of the current binding hypotheses and at a more adequate characterization of the structure−function relationships of the CYP17 and CYP19 P450 enzymes.

Experimental Section

Reagents and General Methods. Chemicals and reagents were obtained from commercial sources and used without further purification. Liquid chromatography was carried out using Merck 60 (0.063−0.200 mm) silica gel. Flash chromatography was performed on Merck 60 (0.015−0.040 mm) according to the procedure of Still.[52] Thin-layer chromatography was carried out on Merck 60 F254 250-μm silica gel plates. Tetrahydrofuran (THF) was distilled under N_2 from sodium/benzophenone ketyl. Melting points were determined by the capillary method on a Stuart Scientific SMP-3 electrothermal apparatus and are uncorrected. Elemental analyses (C, H, and N) were made on an Euroea 3000 analyzer. IR spectra were recorded as KBr pellets on a Perkin-Elmer FT-IR spectrophotometer; only the most significant absorption bands have been reported. ^{1}H NMR spectra were recorded at 300 MHz on a Varian 300 instrument. Chemical shifts are reported in δ (ppm) downfield from an internal solvent peak and coupling costants, J in hertz. OH protons were detected upon proton exchange with D_2O.

Preparation of 7-Hydroxy-8-methyl-2*H*-chromen-2-one. 2-Methylresorcinol (16.5 mmol, 2.0 g) and ethyl 3,3-diethoxypropionate (15 mmol, 3.2 mL) were heated at 120 °C through an external oil bath until a clear solution was formed. The reaction mixture was then cooled to 0 °C, and a mixture of concentrated H_2SO_4 (33 mmol, 1.8 mL) and CF_3COOH (33 mmol, 2.5 mL) was slowly added. After 0.5 h stirring at room temperature, the reaction mixture was poured onto ice and the precipitate was filtered and dried under vacuum to afford 2.6 g (95% yield) of the desired product.^{1}H NMR (DMSO-d_6): δ 2.13 (s, 3H); 6.16 (d, 1H, J = 9.3); 6.82 (d, 1H, J = 8.4); 7.34 (d, 1H, J = 8.4); 7.89 (d, 1H, J = 9.3); 10.43 (s, 1H). IR: cm^{-1} 3444, 1748, 1607, 829.

Preparation of 7-Hydroxy-3-methyl-2*H*-chromen-2-one. A mixture of 2,4-dihydroxybenzaldehyde (21.6 mmol, 3.0 g), sodium propionate (46.8 mmol, 4.5 g), propionic anhydride (58.2 mmol, 7.5 mL), and piperidine (3 mmol, 0.3 mL) was refluxed for 6 h and then poured onto ice. The aqueous mixture, made acidic with a 0.1 N solution of HCl, yielded a precipitate that was filtered and treated under stirring with concentrated H_2SO_4 (2 mL). The resulting mixture was poured onto ice again to afford 2.6 g (71%) of the desired product. ^{1}H NMR (DMSO-d_6): δ 2.01 (s, 3H); 6.70 (d, 1H, J = 1.9); 6.74 (dd, 1H, J = 2.2, 8.5); 7.41 (d, 1H, J = 8.5); 7.73 (s, 1H); 10.35 (s, 1H). IR: cm^{-1} 3242, 1683, 1624, 837.

Preparation of 4-Methyl-7-phenoxy-2*H*-chromen-2-one. Ethyl acetoacetate (21.2 mmol, 3 mL), 3-phenoxyphenol (7.5 mmol, 1.4 g), and a drop of concentrated H_2SO_4 were heated to 120 °C. After 8 h stirring, the solution was poured onto ice and extracted with EtOAc. The organic layer was washed with a saturated solution of $NaHCO_3$ and brine and then dried over Na_2SO_4. The solvent was removed under vacuum, and the residue was purified by column chromatography using $CHCl_3$/hexane 7/3 as eluent to afford an oil, that gave 0.66 g (35%) of a solid upon treatment with a mixture of ether and hexane. ^{1}H NMR ($CDCl_3$): δ 2.40 (s, 3H); 6.17 (s, 1H); 6.85 (d, 1H, J = 2.5); 6.94 (dd, 1H, J = 2.5, 8.8); 7.08 (dd,

2H, J = 1.2, 3.2); 7.38−7.48 (m, 3H); 7.53 (d, 1H, J = 8.8). IR: cm^{-1} 1732, 1614, 844.

Preparation of 7-Hydroxy-3-methyl-4-phenyl-2*H*-chromen-2-one. To a solution of resorcinol (28.8 mmol, 3.2 g) in ethyl 2-methyl-3-oxo-3-phenylpropanoate (26.2 mmol, 5.4 g) was added at 0 °C a mixture of concentrated H_2SO_4 (57.6 mmol, 3.1 mL), and CF_3COOH (57.6 mmol, 4.46 mL). After 4 h stirring at room temperature, the reaction mixture was poured onto ice and extracted with EtOAc. The organic layer was dried over Na_2SO_4 and concentrated under vacuum to afford 5.3 g (80% yield) of the desired product. ^1H NMR (DMSO-d_6): δ 1.78 (s, 3H); 6.78−6.61 (m, 3H); 7.20−7.29 (m, 2H); 7.42−7.57 (m, 3H); 10.40 (s, 1H). IR: cm^{-1} 3144, 1670, 1623, 701.

Preparation of 7-Hydroxy-4-pyridin-4-yl-2*H*-chromen-2-one. A mixture of resorcinol (14.2 mmol, 16 g) and ethyl 3-oxo-3-pyridin-4-ylpropanoate (13 mmol, 2.5 mL) was cooled to 0 °C. To the solution was slowly added a mixture of H_2SO_4 (28.6 mmol, 1.6 mL) and CF_3COOH (28.6 mmol, 2.2 mL). After 1 h stirring at room temperature, the mixture was poured onto ice and then extracted with EtOAc. The organic layer was washed with $NaHCO_3$, dried over Na_2SO_4, and concentrated under vacuum to give upon treatment with ether 0.93 g (30% yield) of the desired product. ^1H NMR (DMSO-d_6): δ 5.27 (s, 1H); 5.78 (d, 1H, J = 2.1); 5.92 (dd, 1H, J = 9.0, 2.2); 6.63 (d, 1H, J = 9.3); 7.40 (d, 2H, J = 6.0); 8.65 (d, 2H, J = 5.8). OH proton was undetectable. IR: cm^{-1} 3441, 1688, 1603, 828.

Preparation of 7-Hydroxy-5-methyl-2*H*-chromen-2-one. 5-Methylresorcinol (56.5 mmol, 8.0 g) and ethyl 3,3-diethoxypropionate (51.4 mmol, 10 mL) were heated to 120 °C through an external oil bath until a clear solution was formed. The reaction mixture was then cooled to 0 °C, and a mixture of concentrated H_2SO_4 (113.1 mmol, 6.0 mL) and CF_3COOH (113 mmol, 8.8 mL) was slowly added. After 3 h stirring at room temperature, the reaction mixture was poured onto ice and the precipitate was filtered and dried under vacuum. The crude material was purified through a column chromatography using $CHCl_3$/AcOEt 1:1 as eluent. 70%, yield. ^1H NMR (DMSO-d_6): δ 2.13 (s, 3H); 6.16 (d, 1H, J = 9.3); 6.82 (d, 1H, J = 8.4); 7.34 (d, 1H, J = 8.4); 7.89 (d, 1H, J = 9.3); 10.43 (s, 1H). IR: cm^{-1} 3444, 1748, 1607, 829.

Preparation of 4-(Chloromethyl)-7-hydroxy-2*H*-chromen-2-one. To a solution of resorcinol (10 mmol, 1.1 g) in 4 mL (29.6 mmol) of ethyl 4-chloro-3-oxobutanoate was added 2 drops of H_2SO_4, followed by stirring at 120 °C for 6 h. The mixture was poured onto ice and extracted with AcOEt. The organic layer was separated and concentrated under vacuum to afford an oil that upon treatment with $CHCl_3$ afforded the desired compound as a white solid, that was used in the next steps without further purification. 25% yield.^1H NMR (acetone-d_6): δ 4.92 (s, 2H); 6.40 (s, 1H); 6.80 (d, 1H, J = 2.5); 6.91 (dd, 1H, J = 8.8, 2.5); 7.72 (d, 1H, J = 8.8); 9.50 (s, 1H). IR: cm^{-1} 3283, 1686, 1625.

Preparation of 4-(Chloromethyl)-2*H*-chromen-2-one. To a solution of phenol (53.1 mmol, 5.0 g) in 2.4 mL (17.7 mmol) of ethyl 4-chloro-3-oxobutanoate was added 6 drops of concentrated H_2SO_4, followed by stirring at 120 °C for 3 h. The reaction mixture was diluted with AcOEt and washed with a saturated solution of K_2CO_3 (3 × 10 mL). The organic layer was separated, dried over Na_2SO_4, and concentrated under vacuum. The oil residue was purified by column chromatography using $CHCl_3$/petroleum ether/AcOEt 5:4:1 as eluent. 20% yield.^1H NMR ($CDCl_3$): δ 4.65 (s, 2H), 6.55 (s, 1H), 7.20−7.80 (m, 4H). IR: cm^{-1} 1710.

Preparation of 7-Benzyloxy-4-(chloromethyl)-2*H*-chromen-2-one. To a solution of 4-(chloromethyl)-7-hydroxy-2*H*-chromen-2-one (1.5 mmol, 0.5 g) in EtOH (15 mL) were added K_2CO_3 (4.5 mmol, 0.6 g) and benzyl bromide (4.5 mmol, 0.5 mL). The reaction was stirred at reflux for 3 h. K_2CO_3 was filtered off and the solution concentrated under vacuum. The oil residue was purified by column chromatography using $CHCl_3$/hexane 9:1 to afford 0.25 g (50% of yield) of desired compound.^1H NMR ($CDCl_3$): δ 4.62 (2 H); 5.14 (s, 2H); 6.40 (d, 1H); 6.92 (d, 1H, J = 2.5); 6.97 (dd, 1H, J = 8.8, 2.5); 7.34−7.45 (m, 5H); 7.57 (d, 1H, J = 8.8). IR: cm^{-1} 1732, 1614.

General Procedure for the Preparation of 7-Methoxycoumarin Derivatives. A suitable 7-hydroxycoumarin derivative (11.3 mmol) was dissolved in DMF (45.4 mL) and the solution cooled to 0 °C. NaH (25 mmol, 0.7 g) was slowly added to the solution followed by 20 min stirring. CH_3I (25 mmol, 0.8 mL) was then added to the reaction mixture that slowly reached room temperature. After 4 h, 25 mmol of NaH and CH_3I were added again to the reaction mixture under stirring. After 1 h, the mixture was poured onto ice and extracted with EtOAc (3 × 10 mL). The organic layer was extracted with a 2 N solution of NaOH (3 × 5 mL) and water (3 × 5 mL), dried over Na_2SO_4, and then concentrated under vacuum to give the desired derivatives described below that were used in the next steps without further purification (unless otherwise indicated):

7-Methoxy-8-methyl-2*H*-chromen-2-one. 36%, yield. ^1H NMR ($CDCl_3$): δ 2.29 (s, 3H); 3.91 (s, 3H); 6.23 (d, 1H, J = 9.3); 6.82 (d, 1H, J = 8.5); 7.28 (d, 1H, J = 8.5); 7.62 (d, 1H, J = 9.3). IR: cm^{-1} 1734, 1609, 885.

7-Methoxy-5-methyl-2*H*-chromen-2-one. The crude material was recrystallized from EtOH. 62%, yield. ^1H NMR ($CDCl_3$): δ 2.47 (s, 3H); 3.85 (s, 3H); 6.25 (d, 1H, J = 9.7); 6.67 (s, 1H); 7.25 (s, 1H); 7.82 (d, 1H, J = 9.7). IR: cm^{-1} 1731, 1621, 873.

7-Methoxy-3-methyl-4-phenyl-2*H*-chromen-2-one. 83%, yield. ^1H NMR ($CDCl_3$): δ 1.95 (s, 3H); 3.85 (s, 3H); 6.69 (dd, 1H, J = 2.5, 9.1); 6.86 (d, 1H, J = 2.5); 6.89 (d, 1H, J = 9.1); 7.17−7.38 (m, 2H); 7.41−7.55 (m, 3H). IR: cm^{-1} 1699, 1613, 700.

7-Methoxy-3-methyl-2*H*-chromen-2-one. 34%, yield. ^1H NMR ($CDCl_3$): δ 2.17 (s, 3H); 3.86 (s, 3H); 6.81−6.83 (m, 2H); 7.30 (d, 1H, J = 9.3); 7.45 (s, 1H). IR: cm^{-1} 1706, 1617, 833.

7-Methoxy-4-pyridin-4-yl-2*H*-chromen-2-one (33). Mp 209−211 °C. 40%, yield. ^1H NMR ($CDCl_3$): 3.89 (s, 3H); 6.22 (s, 1H); 6.82 (dd, 1H, J = 9.79, 2.74); 6.92 (d, 1H, J = 2.48); 7.26 (s, 1H); 7.36 (dd, 2H, J = 4.40, 1.65); 8.80 (dd, 2H, J = 4.12, 1.37). IR: cm^{-1} 1720, 1596. Anal. ($C_{15}H_{11}NO_3$) C, H, N.

General Procedure for the Preparation of Bromomethylcoumarin Derivatives and for the Synthesis of Bromoindenodiazine Derivatives 5 and 9. To the solution of 0.69 mmol of a suitable methylcoumarin derivative (or indenodiazine derivative) in CCl_4 (2.5 mL) were added *N*-bromosuccinimide (0.83 mmol, 0.15 g) and a catalytic amount of benzoyl peroxide or AIBN (**5** and **9**). The reaction mixture was refluxed until the disappearance of the starting material (about 2 h). The succinimide was rapidly filtered off and the desired solid product recovered after cooling and used in the next step without further purification, unless otherwise indicated:

8-(Bromomethyl)-7-methoxy-2*H*-chromen-2-one. 59%, yield. ^1H NMR ($CDCl_3$): δ 4.00 (s, 3H); 4.77 (s, 2H); 6.28 (d, 1H, J = 9.5); 6.86 (d, 1H, J = 8.6); 7.42 (d, 1H, J = 8.6); 7.63 (d, 1H, J = 9.5). IR: cm^{-1}1732, 1607, 999.

5-(Bromomethyl)-7-methoxy-2*H*-chromen-2-one. 51%, yield. ^1H NMR ($CDCl_3$): δ 3.36 (d, 1H, J = 9.6); 3.87 (s, 3H); 4.59 (s, 2H); 6.79 (d, 1H, J = 2.0); 6.86 (d, 1H, J = 2.0); 7.94 (d, 1H, J = 9.6). IR:cm^{-1} 1732, 1602, 829.

3-(Bromomethyl)-7-methoxy-4-phenyl-2*H*-chromen-2-one. 40%, yield. ^1H NMR ($CDCl_3$): δ 3.87 (s, 3H); 4.24 (s, 2H); 6.73 (dd, 1H, J = 8.9, 2.5); 6.87 (d, 1H, J = 2.2); 6.90 (d, 1H, J = 8.9); 7.37 (dd, 2H, J = 2.5, 7.7); 7.53−7.58 (m, 3H). IR: cm^{-1} 1713, 1616, 860.

4-(Bromomethyl)-3-phenyl-2*H*-chromen-2-one. The crude solid was recrystallized from ethanol. 77%, yield. ^1H NMR ($CDCl_3$): δ 4.39 (s, 2H); 7.25 (s, 1H); 7.36−7.58 (m, 7H); 7.81 (dd, 1H, J = 1.4, 7.9). IR: cm^{-1} 3064, 1726, 1604, 762.

6-(Bromomethyl)-2*H*-chromen-2-one. 30%, yield. ^1H NMR ($CDCl_3$): δ 2.77 (s, 2H); 6.45 (d, 1H, J = 9.6); 7.31 (d, 1H. J = 8.5); 7.51−7.57 (m, 2H); 7.68 (d, 1H, J = 9.6). IR: cm^{-1} 3022, 1714, 1620, 822.

3-(Bromomethyl)-7-methoxy-2*H*-chromen-2-one. 35%, yield. ^1H NMR ($CDCl_3$): δ 3.88 (s, 3H); 4.42 (s, 2H); 6.83−

6.88 (m, 2H); 7.39 (d, 1H, $J = 8.5$); 7.78 (s, 1H). IR: cm^{-1} 1699, 1614, 850.

4-(Bromomethyl)-7-phenoxy-2*H*-chromen-2-one. The reaction crude was purified by chromatography using $CHCl_3$/hexane 1:1 as eluent. 40%, yield. ^1H NMR ($CDCl_3$): δ 4.45 (s, 2H); 6.39 (s, 1H); 6.86 (d, 1H, $J = 2.5$); 6.98 (dd, 1H, $J = 2.5$, 8.5); 7.20 (d, 2H, $J = 8.5$); 7.39−7.45 (m, 3H); 7.66 (d, 1H, $J = 8.5$). IR: cm^{-1} 1725, 1614, 843.

7-(Bromomethyl)-2*H*-chromen-2-one. The crude compound was recrystallized from ethanol. 70%, yield.^1H NMR ($CDCl_3$): δ 4.80 (s, 2H), 6.50 (d, 1H, $J = 9.0$), 6.45 (m, 2H), 6.75 (d, 1H, $J = 7.5$), 8.10 (d, 1H, $J = 9.0$). IR: cm^{-1} 1715, 1620.

5-Bromo-2-methyl-5*H*-indeno[1,2-*d*]pyrimidine (5). The crude material was purified by chromatography using EtOAc/hexane 1:1. 70% yield. ^1H NMR ($CDCl_3$) δ 2.84 (s, 3H); 6.02 (s, 1H); 7.50−7.65 (m, 2H); 7.74 (dd, 1H, $J = 8.4$, 0.8); 8.06 (dd, 1H, $J = 6.0$, 1.4); 8.82 (s, 1H). IR: cm^{-1} 1720, 1410.

3-(Bromomethyl)-5*H*-indeno[1,2-*c*]pyridazin-5-one (9). The crude reaction mixture was purified by chromatography using EtOAc/hexane 1:1 as eluent. 50%, yield. ^1H NMR ($CDCl_3$) δ 4.78 (s, 2H); 7.57 (td, 1H, $J = 7.6$, 0.9); 7.74 (td, 1H, $J = 7.4$, 1.1); 7.77 (s, 1H); 7.85 (dd, 1H, $J = 7.8$, 0.8); 8.17 (dd, 1H, $J = 8.0$, 0.8). IR: cm^{-1} 1590, 1420.

General Procedure for the Synthesis of Indenodiazine Derivatives 6, 7, and 10. To a solution of **5** or **9** (2 mmol) in dioxane (8 mL) was added imidazole (6 mmol, 0.41 g), followed by heating at reflux for 1 h until the starting material disappeared. The solvent was removed under vacuum and then dissolved in EtOAc and extracted with a saturated solution of $NaHCO_3$. The organic layer was separated, dried over Na_2SO_4, and concentrated under vacuum. Compounds **6** and **7** were separated and purified through column chromatography (eluent: $CHCl_3$/EtOAc/MeOH 90:5:5).

4-(1*H*-Imidazol-1-yl)-2-methyl-5*H*-indeno[1,2-*d*]pyrimidine (6). 30%, yield. Mp 181−183 °C. ^1H NMR ($CDCl_3$): δ 2.82 (s, 3H); 4.1 (s, 2H); 7.25 (s, 1H); 7.48−7.60 (m, 2H); 7.65 (d, 1H, $J = 7.3$); 7.90 (d, 1H, $J = 1.2$); 8.15 (dd, 1H, $J = 6.9$, 1.1); 8.57 (s, 1H). IR: cm^{-1} 1600, 1580, 1545.

5-(1*H*-Imidazol-1-yl)-2-methyl-5*H*-indeno[1,2-*d*]pyrimidine (7). The crude compound was recrystallized from CH_3CN. 36%, yield. Mp dec 186 °C. ^1H NMR ($CDCl_3$): δ 2.83 (s, 3H); 6.27 (s, 1H); 6.68 (s, 1H); 7.18 (s, 1H); 7.44 (dd, 1H, $J = 7.7$, 1.0); 7.55 (td, 1H, $J = 7.4$, 1.4); 7.59 (td, 1H, $J = 7.3$, 1.1); 7.70 (s, 1H); 8.14 (dd, 1H, $J = 7.7$, 1.0); 8.58 (s, 1H). IR: cm^{-1} 1720, 1410. Anal. ($C_{15}H_{12}N_4$) C, H, N.

3-(1*H*-Imidazol-1-ylmethyl)-5*H*-indeno[1,2-*c*]pyridazin-5-one (10). The crude compound was recrystallized from EtOH. 40%, yield. Mp dec 186 °C. ^1H NMR ($CDCl_3$): δ 5.52 (s, 2H); 7.01 (s, 1H); 7.15 (s, 1H); 7.24 (s, 1H); 7.56 (td, 1H, $J = 7.6$, 0.9); 7.66 (s, 1H); 7.73 (td, 1H, $J = 7.2$, 0.9); 7.82 (d, 1H, $J = 7.3$); 8.15 (d, 1H, $J = 7.7$). IR: cm^{-1} 3090, 1590, 1420. Anal. ($C_{15}H_{10}N_4O$) C, H, N.

Synthesis of 1-(9*H*-Fluoren-9-yl)-1*H*-imidazole (13) and 1-(9-Phenyl-9*H*-fluoren-9-yl)-1*H*-imidazole (14). To a solution of 0.9 mmol of the bromofluorenyl derivatives **11** or **12** in dioxane (5 mL), was added imidazole (2.6 mmol, 0.18 g) followed by heating at reflux for 3 h. The solvent was removed under vacuum. The residue was dissolved in $CHCl_3$ and extracted with a saturated solution of $NaHCO_3$. The organic layer was dried over Na_2SO_4 and concentrated under vacuum. The solid residue was purified by chromatography using $CHCl_3$/CH_3OH 9:1 as eluent. The major isolated product was recrystallized from EtOAc:

1-(9*H*-Fluoren-9-yl)-1*H*-imidazole (13). 60%, yield. Mp 154−155 °C. ^1H NMR ($CDCl_3$): δ 6.10 (s, 1H); 6.68 (s, 1H); 7.03 (s, 1H); 7.20−7.40 (m, 4H); 7.45 (td, 2H, $J = 6.7$, 0.2); 7.67 (s, 1H); 7.75 (d, 2H, $J = 7.6$). IR: cm^{-1} 3090, 1470, 1430. Anal. ($C_{16}H_{12}N_2$) C, H, N.

1-(9-Phenyl-9*H*-fluoren-9-yl)-1*H*-imidazole (14). 42%, yield. Mp 201−202 °C. ^1H NMR (DMSO-d_6): δ 6.99 (m, 1H); 7.08 (m, 1H); 7.12−7.18 (m, 2H); 7.26−7.32 (m, 5H); 7.39−7.46 (m, 4H); 7.51−7.55 (m, 1H); 7.72 (s, 1H); 7.76 (s, 1H). IR: cm^{-1} 1480, 1450. Anal. ($C_{22}H_{16}N_2$) C, H, N.

General Procedure for the Synthesis of Fluorenyltriazole Derivatives 15−17. Anhydrous DMF (5 mL) was added under argon to NaH (11.7 mmol, 0.28 g). To the mixture was added 1*H*-1,2,4-triazole or 1*H*-1,2,3-triazole (9.4 mmol), followed by careful heating until cessation of the gas evolution. Compound **11** (2.3 mmol, 0.8 g) was added, and the reaction mixture was stirred at 90 °C for 3 h. The solvent was removed under vacuum. The residue was dissolved in EtOAc, washed with water, dried over Na_2SO_4, and concentrated under vacuum. Title compounds **15** and **17** were obtained through a chromatographic separation (eluent: hexane/EtOAc/2-propanol 7.5:2.5:0.5) of the reaction mixture and recrystallized from EtOAc:

4-(9-Phenyl-9*H*-fluoren-9-yl)-4*H*-1,2,4-triazole (15). 21%, yield. Mp 220−221 °C. ^1H NMR (DMSO-d_6): δ 7.13−7.19 (m, 2H); 7.35−7.40 (m, 3H); 7.42 (td, 2H, $J = 7.6$, 0.9); 7.54 (td, 2H, $J = 7.4$, 0.9); 7.66 (s, 1H); 7.68 (s, 1H); 7.94 (s, 1H); 7.98 (s, 1H); 8.32 (s, 2H). IR: cm^{-1} 3107, 1491, 1451. Anal. ($C_{21}H_{15}N_2$) C, H, N.

1-(9-Phenyl-9*H*-fluoren-9-yl)-1*H*-1,2,3-triazole (16). 43%, yield. Mp 210−211 °C. ^1H NMR (DMSO-d_6): δ 6.87−6.90 (m, 2H); 7.29−7.32 (m, 3H); 7.38 (td, 2H, $J = 7.5$, 1.0); 7.51 (td, 2H, $J = 7.5$, 1.0); 7.63 (s, 1H); 7.66 (s, 1H); 7.78 (s, 1H); 7.95 (s, 1H); 7.97 (s, 1H); 8.09 (s, 1H). IR: cm^{-1} 3158, 1489, 1450. Anal. ($C_{21}H_{15}N_2$) C, H, N.

1-(9-Phenyl-9*H*-fluoren-9-yl)-1*H*-1,2,4-triazole (17). 30%, yield. Mp 239−240 °C. ^1H NMR (DMSO-d_6): δ 6.92−6.98 (m, 2H); 7.27−7.32 (m, 3H); 7.39 (td, 2H, $J = 7.6$, 1.0); 7.52 (td, 2H, $J = 7.6$, 1.0); 7.70 (s, 1H); 7.72 (d, 1H, $J = 0.9$); 7.92 (d, 1H, $J = 0.9$); 7.94 (d, 1H, $J = 0.9$); 8.00 (s, 1H); 8.22 (s, 1H). IR: cm^{-1} 3149, 1497, 1449. Anal. ($C_{21}H_{15}N_2$) C, H, N.

General Procedure for the Preparation of (1*H*-Imidazol-1-ylmethyl)coumarin Derivatives (18−20, 24−27, 30−32, 34). To a solution of imidazole (1.2 mmol, 83 mg) in THF (2 mL) were added K_2CO_3 (2.4 mmol, 0.33 g) and 0.41 mmol of a suitable bromo(or chloro)methylcoumarin derivatives. The reaction mixture was refluxed for 5−7 h, the K_2CO_3 was filtered, and the solution was concentrated under vacuum. The crude residue was recrystallized from ethanol, unless otherwise stated.

3-(1*H*-Imidazol-1-ylmethyl)-7-methoxy-2*H*-chromen-2-one (18). The crude residue was purified by flash chromatography using $CHCl_3$/CH_3OH 97.5:2.5. Finally, the product was recrystallized from $CHCl_3$/hexane. 42%, yield. Mp 136−138 °C. ^1H NMR ($CDCl_3$): δ 3.87 (s, 3H); 5.04 (s, 2H); 6.83−6.86 (m, 2H); 7.02 (s, 1H); 7.14 (s, 2H); 7.30 (d, 1H, $J = 8.5$); 7.62 (s, 1H). IR: cm^{-1} 1705, 1610, 817. Anal. ($C_{14}H_{12}N_2O_3$) C, H, N.

4-(1*H*-Imidazol-1-ylmethyl)-2*H*-chromen-2-one (19). The crude residue was purified by flash chromatography using $CHCl_3$/CH_3OH 9:1 as eluent, then recrystallized from $CHCl_3$/hexane. 50%, yield. Mp 179−180 °C. ^1H NMR (DMSO-d_6): δ 5.58 (s, 2H); 5.60 (s, 1H); 6.99 (s, 1H); 7.27 (s, 1H); 7.40 (t, 1H, $J = 7.9$); 7.44 (d, 1H, $J = 8.4$); 7.66 (td, 1H, $J = 7.9$, 1.5); 7.80 (s, 1H); 7.85 (dd, 1H, $J = 7.9$, 1.5). IR: cm^{-1} 1709, 1608. Anal. ($C_{13}H_{10}N_2O_2$) C, H, N.

4-(1*H*-Imidazol-1-ylmethyl)-7-methoxy-2*H*-chromen-2-one (20). 40%, yield. Mp 176−177 °C. ^1H NMR (DMSO-d_6): δ 3.85 (s, 3H); 5.42 (s, 1H); 5.52 (s, 2H); 6.98−7.05 (m, 3H); 7.26 (s, 1H); 7.75 (s, 1H); 7.74−7.84 (m, 1H). IR: cm^{-1} 1704, 1620, 1610. Anal. ($C_{14}H_{12}N_2O_3$) C, H, N.

4-(1*H*-Imidazol-1-ylmethyl)-7-phenoxy-2*H*-chromen-2-one (24). The reaction crude was purified by column chromatography using EtOAc/$CHCl_3$ 7:3 as eluent. The oil residue afford a solid upon treatment with a solution of ether and ethanol. 40%, yield. Mp 150−151 °C. ^1H NMR ($CDCl_3$): δ 5.28 (s, 2H); 5.75 (s, 1H); 6.88 (d, 1H, $J = 2.5$); 6.94−6.97 (m, 2H); 7.07−7.10 (m, 2H); 7.19 (s, 1H); 7.20−7.30 (1H, partially masked by the solvent peak); 7.43−7.45 (m, 3H); 7.59 (s, 1H). IR: cm^{-1} 1725, 1616, 849. Anal. ($C_{19}H_{14}N_2O_3$) C, H, N.

5-(1*H*-Imidazol-1-ylmethyl)-7-methoxy-2*H*-chromen-2-one (25). 43%, yield. Mp 139−140 °C. ^1H NMR ($CDCl_3$): δ 3.82 (s, 3H); 5.25 (s, 2H); 6.29 (d, 1H, $J = 7.5$); 6.50 (s,

1H); 6.80 (s, 1H); 6.89 (s, 1H); 7.89 (d, 1H, J = 7.5); 7.12 (s, 1H); 7.52 (s, 1H). IR: cm^{-1} 1733, 1603. Anal. ($C_{14}H_{12}N_2O_3$) C, H, N.

6-(1*H*-Imidazol-1-ylmethyl)-2*H*-chromen-2-one (26). The reaction crude was purified by flash chromatography using $CHCl_3$/CH_3OH 9:1 as eluent. The product was finally recrystallized from ether. 44%, yield. Mp 89−90 °C. ^{1}H NMR ($CDCl_3$): δ 5.19 (s, 2H); 6.45 (d, 1H, J = 9.6); 6.91 (s, 1H); 7.12 (s, 1H); 7.20 (s, 1H); 7.34 (s, 2H); 7.58 (s, 1H); 7.67 (d, 1H, J = 9.6). IR: cm^{-1} 1717, 1625, 830. Anal. ($C_{13}H_{10}N_2O_2$) C, H, N.

7-(1*H*-Imidazol-1-ylmethyl)-2*H*-chromen-2-one (27). 52%, yield. Mp 171−172 °C. ^{1}H NMR (DMSO-d_6): δ 5.21 (s, 2H); 6.43 (d, 1H, J = 9.6); 6.91 (s, 1H); 7.00 (dd, 1H, J = 7.8, 1.1); 7.11 (s, 1H); 7.13 (s, 1H); 7.46 (d, 1H, J = 7.8); 7.57 (s, 1H); 7.68 (d, 1H, J = 9.6). IR: cm^{-1} 1713, 1617. Anal. ($C_{13}H_{10}N_2O_2$) C, H, N.

8-(1*H*-Imidazol-1-ylmethyl)-7-methoxy-2*H*-chromen-2-one (30). The reaction crude was purified by column chromatography using $CHCl_3$/CH_3OH 95:5 as eluent. 40%, yield. Mp dec 250 °C. ^{1}H NMR ($CDCl_3$): δ 3.98 (s, 3H); 5.34 (s, 2H); 6.28 (d, 1H, J = 9.6); 6.87 (d, 1H, J = 8.8); 6.97 (s, 1H); 7.11 (s, 1H); 7.44 (d, 1H, J = 8.8); 7.63 (d, 1H, J = 9.6); 7.67 (s, 1H). IR: cm^{-1} 1727, 1609, 840. Anal. ($C_{14}H_{12}N_2O_3$) C, H, N.

4-(1*H*-Imidazol-1-ylmethyl)-3-phenyl-2*H*-chromen-2-one (31). 52%, yield. Mp 216−218 °C. ^{1}H NMR ($CDCl_3$): δ 5.15 (s, 2H); 6.80 (s, 1H); 7.03 (s, 1H); 7.26−7.31 (m, 3H); 7.38−7.60 (m, 7H). IR: cm^{-1} 1710, 1603, 756. Anal. ($C_{19}H_{14}N_2O_2$) C, H, N.

3-(1*H*-Imidazol-1-ylmethyl)-7-methoxy-4-phenyl-2*H*-chromen-2-one (32). The reaction crude was purified by chromatography using $CHCl_3$/EtOAc 9:1. 60%, yield. Mp 114−116 °C. ^{1}H NMR ($CDCl_3$): δ 3.87 (s, 3H); 4.84 (s, 2H); 6.73 (dd, 1H, J = 2.6, 8.9); 6.86−6.93 (m, 4H); 7.18−7.21 (m, 3H); 7.57−7.60 (m, 3H). IR: cm^{-1} 1709, 1615, 833. Anal. ($C_{20}H_{16}N_2O_3$) C, H, N.

7-Benzyloxy-4-(1*H*-imidazol-1-ylmethyl)-2*H*-chromen-2-one (34). The reaction crude was purified by chromatography using $CHCl_3$/MeOH 9:1. 50%, yield. Mp 172−173 °C. ^{1}H NMR (DMSO-d_6): δ 5.23 (s, 2H); 5.42 (s, 1H); 5.52 (s, 2H); 6.97 (s, 1H); 7.07 (d, 1H, J = 8.8); 7.12 (d, 1H, J = 2.1); 7.26 (s, 1H); 7.33−7.47 (m, 5H); 7.75−7.78 (m, 2H). IR: cm^{-1} 1700, 1610. Anal. ($C_{20}H_{16}N_2O_3$) C, H, N.

Preparation of 6-(1*H*-Imidazol-1-ylmethyl)-2*H*-chromene-2-thione (35). To a solution of derivative **26** (0.2 mmol, 0.04 g) in toluene (0.5 mL) was added Lawesson's reagent (0.1 mmol, 0.04 g), followed by heating at reflux for 4 h under argon atmosphere. The solvent was removed under vacuum and the mixture purified by column chromatography using $CHCl_3$/MeOH 9:1 as eluent. 10% yield. Mp 98 °C dec ^{1}H NMR ($CDCl_3$): δ 5.20 (s, 2H); 6.91 (d, 1H, J = 1.1); 7.14 (s, 1H); 7.15−7.24 (m, 2H); 7.35−7.40 (m, 2H); 7.43 (d, 1H, J = 8.0); 7.60 (s, 1H). IR: cm^{-1} 1755, 1457, 1250. Anal. ($C_{13}H_{10}N_2OS$) C, H, N.

Preparation of 7-Methoxy-4-(1*H*-1,2,4-triazol-1-ylmethyl)-2*H*-chromen-2-one (21). To a solution of 1*H*-1,2,4-triazole (4 mmol, 0.28 g) in THF (7 mL) were added K_2CO_3 (4 mmol, 0.55 g), 4-(bromomethyl)-7-methoxy-2*H*-chromen-2-one (1.3 mmol, 0.36 g), and a catalytic amount of TBAI. The reaction mixture was refluxed for 2 h, K_2CO_3 was filtered off, and the solution was concentrated under vacuum. The crude residue was recrystallized from ethanol. 45%, yield. Mp 182−183 °C. ^{1}H NMR (DMSO-d_6): δ 3.84 (s, 3H); 5.63 (s, 1H); 5.74 (s, 2H); 6.98 (dd, 1H, J = 8.8, 2.5); 7.03 (d, 1H, J = 2.5); 7.76 (d, 1H, J = 8.8); 8.08 (s, 1H); 8.71 (s, 1H). IR: cm^{-1} 1703, 1610. Anal. ($C_{13}H_{11}N_3O_3$) C, H, N.

Preparation of 7-(1*H*-1,2,4-Triazol-1-ylmethyl)-2*H*-chromen-2-one (28). To a solution of 1*H*-1,2,4-triazole (6.3 mmol, 0.43 g) in THF (10.5 mL) were added K_2CO_3 (6.3 mmol, 0.87 g) and 7-(bromomethyl)-2*H*-chromen-2-one (2.1 mmol, 0.5 g). The reaction mixture was refluxed for 2 h, K_2CO_3 was filtered off, and the solution was concentrated under vacuum. The crude residue was recrystallized from ethanol. 48%, yield. Mp 201−202 °C. ^{1}H NMR (DMSO-d_6): δ 5.52 (s, 2H); 6.46 (d, 1H, J = 9.5); 7.20 (dd, 1H, J = 7.9, 1.6); 7.26 (s, 1H); 7.68 (d, 1H, J = 7.9); 8.00 (s, 1H); 8.02 (d, 1H, J = 9.5); 8.68 (s, 1H). IR: cm^{-1} 1732, 1620. Anal. ($C_{12}H_9N_3O_2$) C, H, N.

General Procedure for the Preparation of (2-Bromoethoxy)coumarin Derivatives. To a solution of commercially available 4-hydroxy-7-methoxycoumarin or 4-hydroxycoumarin (5.2 mmol) in THF (26 mL) were added under stirring K_2CO_3 (31.2 mmol, 4.3 g), dibromoethane (2.6 mmol, 0.22 mL), and a catalytic amount of TBAI. The reaction mixture was refluxed for 2 h, the K_2CO_3 filtered off, and the remaining solution concentrated under vacuum and worked up as follows:

4-(2-Bromoethoxy)-2*H*-chromen-2-one. The crude residue was purified by column chromatography using $CHCl_3$/Et_2O/EtOAc 6:3:1. 57%, yield. ^{1}H NMR (DMSO-d_6): δ 3.85 (t, 2H, J = 7.3); 4.60 (t, 2H, J = 7.3); 5.72 (s, 1H); 7.30−7.50 (m, 2H); 7.60−7.80 (m, 1H); 8.2 (d, 1H, J = 8.1). IR: cm^{-1} 1721, 1607.

4-(2-Bromoethoxy)-7-methoxy-2*H*-chromen-2-one. The crude residue was recrystallized from ethanol. 44%, yield. ^{1}H NMR ($CDCl_3$): δ 3.74 (t, 2H, J = 6.1); 3.87 (s, 3H); 4.42 (t, 2H, J = 6.1); 5.53 (s, 1H); 6.80 (s, 1H); 6.85 (d, 1H, J = 8.7); 7.75 (d, 1H, J = 8.7). IR: cm^{-1} 1703, 1621, 814.

7-(2-Bromoethoxy)-2*H*-chromen-2-one. The crude residue was purified by chromatography using $CHCl_3$/Et_2O/EtOAc 6/3/1. 50%, yield. ^{1}H NMR (DMSO-d_6): δ 3.70 (t, 2H, J = 7.5); 4.40 (t, 2H, J = 7.5); 6.32 (d, 1H, J = 10.5); 6.87 (m, 2H); 7.50 (d, 1H, J = 9.0); 7.75 (d, 1H, J = 10.5). IR: cm^{-1} 1720, 1615.

General procedure for the synthesis of compounds 22, 23 and **29.** To a solution of a suitable 2-bromoethoxy derivative (0.5 mmol) in THF (2.5 mL) were added under stirring imidazole (1.5 mmol, 0.1 g), K_2CO_3 (1.5 mmol, 0.2 g), and a catalytic amount of TBAI. The reaction mixture was refluxed for 5 h and then filtered, concentrated under vacuum, and worked-up as follows:

4-[2-(1*H*-Imidazol-1-yl)ethoxy]-2*H*-chromen-2-one (22). The crude residue was purified by column chromatography using $CHCl_3$/CH_3OH 9:1 as eluent and the major isolated compound recrystallized from $CHCl_3$/hexane. 60%, yield. Mp 149−150 °C. ^{1}H NMR (DMSO-d_6): δ 4.48 (s, 4H); 5.90 (s, 1H); 6.90 (s, 1H); 7.29−7.38 (m, 3H); 7.61−7.67 (m, 1H); 7.76−7.80 (m, 2H). IR: cm^{-1} 1723, 1624. Anal. ($C_{14}H_{12}N_2O_3$) C, H, N.

4-[2-(1*H*-Imidazol-1-yl)ethoxy]-7-methoxy-2*H*-chromen-2-one (23). The reaction crude was purified by chromatography using $CHCl_3$/EtOAc 1:1 as eluent. 55%, yield. Mp 139−141 °C. ^{1}H NMR (DMSO-d_6): δ 3.82−3.87 (m, 7H); 6.50 (s, 1H); 7.01 (dd, 1H, J = 2.2, 9.1); 7.16 (d, 1H, J = 2.4); 7.23 (s, 1H); 7.47 (d, 1H, J = 9.1); 7.69 (s, 1H); 8.15 (s, 1H). IR: cm^{-1} 1726, 1610, 837. Anal. ($C_{15}H_{14}N_2O_4$) C, H, N.

7-[2-(1*H*-Imidazol-1-yl)ethoxy]-2*H*-chromen-2-one (29). The crude residue was purified by column chromatography using $CHCl_3$/CH_3OH 95:5 as eluent. The major isolated product was recrystallized from $CHCl_3$/CH_3OH/hexane. 77%, yield. Mp 177−178 °C. ^{1}H NMR (DMSO-d_6): δ 4.34−4.42 (m, 4H); 6.28 (d, 1H, J = 9.4); 6.87 (s, 1H); 6.92 (dd, 1H, J = 8.6, 2.5); 6.99 (d, 1H, J = 2.5); 7.23 (s, 1H), 7.60 (d, 1H, J = 8.6); 7.67 (s, 1H); 7.96 (d, 1H, J = 9.4). IR: cm^{-1} 1721, 1625. Anal. ($C_{14}H_{12}N_2O_3$) C, H, N.

Biological Assays. As source of the enzymes the following microsomal preparations were used: for CYP19, human placenta;[45,46] for CYP17, human testes,[47] or *E.coli*-expressing human CYP17.[48] The CYP19 assay was performed as described using the ^3H_2O method: either [1β,2β-^{3}H] testosterone/testosterone (2.5 μM)[b] or [1β-^{3}H]androstenedione/androstenedione (0.5 μM)[47] were used as substrates. The CYP17 assay was performed with nonlabeled progesterone and an HPLC procedure was employed for the separation of the substrate and androstenedione using UV detection.[47,48]

Computational Studies. Computational studies were performed on a SGI O2 workstation using the molecular modeling packages SYBYL 6.9.2[53] and FloPlus 8.02.[54] Statistical data analyses of CoMFA fields were carried out with the GOLPE 4.5.12[55] program.

Three-dimensional models of all the molecules were built by assembling fragments from the standard fragment library of SYBYL. The flexibility of the substituents was taken into

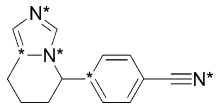

Figure 4.

account by performing a Monte Carlo (MC) conformational search within the QXP program of FloPlus. AM1-ESP charges were calculated using the MOPAC AM1 Hamiltonian implemented in SYBYL.

Structure Alignment. *S*-Fadrozole, (5-(*S*)-phenyl-5,6,7,8-tetrahydroimidazo[1,5-*a*]pyridine), a strong AR inhibitor with a rigid structure of known stereochemistry, was chosen as the template for the alignment, in analogy with some previously published CoMFA of AR inhibitors.[26] Initial energy minimizations were performed with MAXIMIN2 (Tripos Force Field) with partial electrostatic charges calculated by the Marsili−Gasteiger method within Sybyl. The conformational space of each molecule was sampled during the template fitting procedure by means of the TFIT module of QXP. In such a procedure, MC-like searches are adopted to match molecules to the template using a superposition force field which automatically assigns short-range attractive forces to similar atoms in different molecules. In particular, according to a known pharmacophoric hypothesis, five anchoring points of the template, indicated by an asterisk in Figure 4, were chosen to drive the TFIT procedure throughout 1000 runs of MC simulation followed by conjugate gradient minimization.

Three atoms in the five-membered heterocyclic ring, including the nitrogen atom likely coordinating the porphyrinic iron, the carbon atom of the phenyl ring in para position with respect to the cyano group and the nitrogen atom of the cyano group, were chosen. The latter, according to the pharmacophoric hypotheses, should behave as a hydrogen bond (HB) acceptor.

The fitting points in the molecules of our data set were the corresponding atoms in the imidazole or triazole rings, a carbon atom two bonds away from the azole ring and an oxygen atom able to mimic the HB acceptor function of the cyano group in *S*-fadrozole. While the first four atoms could be selected in a unique way, the selection among the oxygen atoms was made taking into account their spatial distance from the nitrogen supposedly coordinating the iron ion. In such a way, one of the two oxygens of the lactone functionality or the ethereal oxygen attached to the benzene ring of the coumarin moiety could be alternatively selected during the overlay process. The imidazole ring of the fluorenyl and indenodiazine derivatives were similarly aligned onto the template. For inhibitor **7**, both enantiomers were used in two separate CoMFA runs and the one better fitted, that was the enantiomer with the *R* absolute configuration, was retained, arbitrarily, for the final analysis.

The selection of the final conformers to be submitted to the CoMFA runs was made looking for the maximum consistency of the aligned molecules. When necessary, different energetically allowed conformers were tested and the ones yielding the most statistically significant PLS models were finally chosen. Prior to the CoMFA runs, the geometry of all the molecules was further refined at a semiempirical level with the AM1 Hamiltonian.

CoMFA/GOLPE Analysis. For the calculation of the 3D QSAR interaction fields, a 3D cubic lattice extending 4 Å beyond all the axes of all the investigated molecules, was automatically created, and a grid spacing of 1 Å was generated. Lennard−Jones 6−12 and Coulomb potentials were employed to calculate the CoMFA steric and electrostatic fields, respectively. A sp^3 carbon atom with a charge of +1 was used as the probe atom. Default settings were used except for the option "drop electrostatic" which was set to "NO", meaning that the electrostatic field was calculated at grid points with high electrostatic interactions (Δ30 kcal/mol). Statistical data treatment for variable selection and for the validation and improved interpretation of the PLS models were performed by means of GOLPE.[55] The field data matrix was imported from SYBYL, and an advanced data pretreatment was performed with GOLPE in order to select unbiased variables by zeroing the negative and positive ones and applying a standard deviation cutoff in order to reduce them to a suitable size. The smart region define (SRD) algorithm was used with the default settings, followed by two consecutive Fractional Factorial Design (FFD) for the final variable selection. By applying all the above data treatments, the original 16566 variables imported from SYBYL were reduced to 882 (63% from the steric and 37% from the electrostatic fields).

Acknowledgment. The Italian authors are indebted to the Italian Ministry for Education, Universities and Research (Rome, Italy) and the German authors to the Fonds der Chemischen Industrie for the financial support. Dr. Angela Rao wishes to thank the Bonino-Pulejo Foundation for supporting her work with a fellowship.

References

(1) Brueggemeier, R. W. Aromatase inhibitors in breast cancer therapy. *Expert. Rev. Anticancer Ther.* **2002**, *2*, 181−191.
(2) Brueggemeier, R. W.; Richards, J. A.; Joomprabutra, S.; Bhat, A. S.; Whetstone, J. L. Molecular pharmacology of aromatase and its regulation by endogenous and exogenous agents. *J. Steroid Biochem. Mol. Biol.* **2001**, *79*, 75−84.
(3) Miller, W. R. Aromatase inhibitors in the treatment of advanced breast cancer. *Cancer Treat. Rev.* **1989**, *16*, 83−93.
(4) Banting, L.; Nicholls, P. J.; Shaw, M. A.; Smith, H. J. Recent developments in aromatase inhibition as a potential treatment for oestrogen-dependent breast cancer. *Prog. Med. Chem.* **1989**, *26*, 253−298.
(5) Lonard, D. M.; Smith, C. L. Molecular perspectives on selective estrogen receptor modulators (SERMs): progress in understanding their tissue-specific agonist and antagonist actions. *Steroids* **2002**, *67*, 15−24.
(6) Park, W. C.; Jordan, V. C. Selective estrogen receptor modulators (SERMs) and their roles in breast cancer prevention. *Trends Mol. Med.* **2002**, *8*, 82−88.
(7) Nicholls, H. Aromatase inhibitors continue their ATAC on tamoxifen. *Trends Mol. Med.* **2002**, *8*, S12−S13.
(8) Miller, W. R. Biological rationale for endocrine therapy in breast cancer. *Best. Pract. Res. Clin. Endocrinol. Metab.* **2004**, *18*, 1−32.
(9) Miller, W. R. Aromatase inhibitors: mechanism of action and role in the treatment of breast cancer. *Semin. Oncol.* **2003**, *30*, 3−11.
(10) Buzdar, A. U. Aromatase inhibitors in breast cancer therapy. *Clin. Breast Cancer* **2003**, *4 Suppl 2*, S84−S88.
(11) Recanatini, M.; Cavalli, A.; Valenti, P. Nonsteroidal aromatase inhibitors: recent advances. *Med. Res. Rev.* **2002**, *22*, 282−304.
(12) Malini, B.; Purohit, A.; Ganeshapillai, D.; Woo, L. W.; Potter, B. V.; Reed, M. J. Inhibition of steroid sulphatase activity by tricyclic coumarin sulphamates. *J. Steroid Biochem. Mol. Biol.* **2000**, *75*, 253−258.
(13) Ahmed, S.; James, K.; Owen, C. P. Inhibition of estrone sulfatase (ES) by derivatives of 4-[(aminosulfonyl)oxy] benzoic acid. *Biorg. Med. Chem. Lett.* **2002**, *12*, 2391−2394.
(14) Pasqualini, J. R.Chetrite, G. S. Estrone sulfatase versus estrone sulfotransferase in human breast cancer: potential clinical applications. *J. Steroid Biochem. Mol. Biol.* **1999**, *69*, 287−292.
(15) Suzuki, T.; Miki, Y.; Nakata, T.; Shiotsu, Y.; Akinaga, S.; Inoue, K.; Ishida, T.; Kimura, M.; Moriya, T.; Sasano, H. Steroid sulfatase and estrogen sulfotransferase in normal human tissue and breast cancer. *J. Steroid Biochem. Mol. Biol.* **2003**, *86*, 449−454.
(16) Santen, R. J.; Samojlik, E.; Lipton, A.; Harvey, H.; Ruby, E. B.; Wells, S. A.; Kendall, J. Kinetic, hormonal and clinical studies with aminoglutethimide in breast cancer. *Cancer* **1977**, *39*, 2948−2958.
(17) Mokbel, K. The evolving role of aromatase inhibitors in breast cancer, *Int J Clin Oncol* **2002**, *7*, 279−283.
(18) Wong, Z. W.Ellis, M. J. First-line endocrine treatment of breast cancer: aromatase inhibitor or antioestrogen? *Br. J. Cancer* **2004**, *90*, 20−25.
(19) Milla-Santos, A.; Milla, L.; Portella, J.; Rallo, L.; Pons, M.; Rodes, E.; Casanovas, J.; Puig-Gali, M. *Anastrozole* versus *tamoxifen* as first-line therapy in postmenopausal patients with hormone-dependent advanced breast cancer: a prospective, randomized, phase III study. *Am. J. Clin. Oncol.* **2003**, *26*, 317−322.
(20) Arora, A.; Potter, J. F. Aromatase inhibitors: current indications and future prospects for treatment of postmenopausal breast cancer. *J. Am. Geriatr. Soc.* **2004**, *52*, 611−6.
(21) Goss, P. E. Risks versus benefits in the clinical application of aromatase inhibitors. *Endocr. Relat. Cancer* **1999**, *6*, 325−32.

(22) Hartmann, R. W.; Ehmer, P. B.; Haidar, S.; Hector, M.; Jose, J.; Klein, C. D.; Seidel, S. B.; Sergejew, T. F.; Wachall, B. G.; Wachter, G. A.; Zhuang, Y. Inhibition of CYP 17, a new strategy for the treatment of prostate cancer. *Arch. Pharm. (Weinheim)*. **2002**, *335*, 119−28.
(23) Clement, O. O.; Freeman, C. M.; Hartmann, R. W.; Handratta, V. D.; Vasaitis, T. S.; Brodie, A. M.; Njar, V. C. Three-dimensional pharmacophore modeling of human CYP17 inhibitors. Potential agents for prostate cancer therapy. *J. Med. Chem.* **2003**, *46*, 2345−2351.
(24) Haidar, S.; Ehmer, P. B.; Hartmann, R. W. Novel steroidal pyrimidyl inhibitors of P450 17 (17 alpha-hydroxylase/C17−20-lyase). *Arch. Pharm. (Weinheim)* **2001**, *334*, 373−374.
(25) Lang, M.; Batzl, C.; Furet, P.; Bowman, R.; Hausler, A.; Bhatnagar, A. S. Structure−activity relationships and binding model of novel aromatase inhibitors. *J. Steroid Biochem. Mol. Biol.* **1993**, *44*, 421−428.
(26) Recanatini, M.; Cavalli, A. Comparative molecular field analysis of non-steroidal aromatase inhibitors: an extended model for two different structural classes. *Bioorg. Med. Chem.* **1998**, *6*, 377−388.
(27) Cavalli, A.; Greco, G.; Novellino, E.; Recanatini, M. Linking CoMFA and protein homology models of enzyme−inhibitor interactions: an application to non-steroidal aromatase inhibitors. *Bioorg. Med. Chem.* **2000**, *8*, 2771−2780.
(28) Cavalli, A.; Recanatini, M. Looking for selectivity among cytochrome P450s inhibitors. *J. Med. Chem.* **2002**, *45*, 251−254.
(29) Sumitomo Chemical Co., Ltd., Japan N-Substituted imidazoles JP Patent 56077263, 1981.
(30) Hirsh, K. S.; Taylor, H. M. Method of inhibiting aromatase and treating estrogen-dependent diseases with azole derivatives. US Patent 4757082, 1988.
(31) Kneubuhler, S.; Thull, U.; Altomare, C.; Carta, V.; Gaillard, P.; Carrupt, P. A.; Carotti, A.; Testa, B. Inhibition of monoamine oxidase-B by 5H-indeno[1,2-c]pyridazines: biological activities, quantitative structure−activity relationships (QSARs) and 3D-QSARs. *J. Med. Chem.* **1995**, *38*, 3874−3883.
(32) Altomare, C.; Cellamare, S.; Summo, L.; Catto, M.; Carotti, A. Inhibition of monoamine oxidase-B by condensed pyridazines and pyrimidine: effects of lipophilicity and structure−activity relationships. *J. Med. Chem.* **1998**, *41*, 3812−3820.
(33) Recanatini, M.; Bisi, A.; Cavalli, A.; Belluti, F.; Gobbi, S.; Rampa, A.; Valenti, P.; Palzer, M.; Palusczak, A.; Hartmann, R. W. A new class of nonsteroidal aromatase inhibitors: design and synthesis of chromone and xanthone derivatives and inhibition of the P450 enzymes aromatase and 17 alpha-hydroxylase/C17,20-lyase. *J. Med. Chem.* **2001**, *44*, 672−680.
(34) Wachter, G. A.; Hartmann, R. W.; Sergejew, T.; Grun, G. L.; Ledergerber, D. Tetrahydronaphthalenes: influence of heterocyclic substituents on inhibition of steroid enzymes P450 arom and P450 17. *J. Med. Chem.* **1996**, *39*, 834−841.
(35) Murray, R. D. The naturally occurring coumarins. *Fortschr. Chem. Org. Naturst*. **2002**, *83*, 1.
(36) Houlr, J. R. S.; Paya, M. Pharmacological and biochemical actions of simple coumarins: natural products with therapeutic potential. *Gen. Pharmacol*. **1996**, *27*, 713−732
(37) Kennedy, R. O.; Thornes, R. D., Eds. *Coumarins: biology, applications and mode of actions*; John Wiley and Sons: Chichester, 1997.
(38) Carotti, A.; Carrieri, A.; Chimichi, S.; Boccalini, M.; Cosimelli, B.; Gnerre, C.; Carotti, A.; Carrupt, P. A.; Testa, B. Natural and synthetic geiparvarins are strong and selective MAO-B inhibitors. Synthesis and SAR studies. *Bioorg. Med. Chem. Lett.* **2002**, *12*, 3551−3555.
(39) Gnerre, C.; Catto, M.; Leonetti, F.; Weber, P.; Carrupt, P. A.; Altomare, C.; Carotti, A.; Testa, B. Inhibition of monoamine oxidases by functionalized coumarin derivatives: biological activities, QSARs, and 3D-QSARs. *J. Med. Chem.* **2000**, *43*, 4747−4758.
(40) Bruhlmann, C.; Ooms, F.; Carrupt, P. A.; Testa, B.; Catto, M.; Leonetti, F.; Altomare, C.; Carotti, A. Coumarins derivatives as dual inhibitors of acetylcholinesterase and monoamine oxidase. *J. Med. Chem.* **2001**, *44*, 3195−3198.
(41) Hirsh, J.; Dalen, J.; Anderson, D. R.; Poller, L.; Bussey, H.; Ansell, J.; Deykin, D. Oral anticoagulants: mechanism of action, clinical effectiveness, and optimal therapeutic range. *Chest.* **2001**, *119(1 Suppl)*, 8S-21S.
(42) Sethna, S.; Phadke, R. The Pechmann reaction. *Org. React.* **1953**, *7*, 1−58.
(43) von Pechmann, H.; Duisberg, C. Über die verbindungen der Phenole mit Acetessigäther. *Chem. Ber.* **1883**, *16*, 2119−2128.
(44) Gadre, J. N.; Audi, A. A.; Karambelkar, N. P. New routes for the synthesis of some hydroxy 2*H*-1-benzopyran-2-thione derivatives. *Indian J. Chem.* **1996**, *35B*, 60−62.
(45) Thompson, E. A., Jr.; Siiteri, P. K. Utilization of oxygen and reduced nicotinamide adenine dinucleotide phophate by human placental microsomes during aromatization of androstenedione. *J. Biol. Chem.* **1974**, *249*, 5364−5372.
(46) Hartmann, R. W.; Batzl, C. Aromatase inhibitors. Synthesis and evaluation of mammary tumor inhibiting activity of 3-alkylated 3-(4-aminophenyl)piperidine-2,6-diones. *J. Med. Chem.* **1986**, *29*, 1362−1369.
(47) Hutschenreuter, T. U.; Ehmer, P. B.; Hartmann, R. W. Synthesis of hydroxy derivates of highly potent non-steroidal CYP17 inhibitors as potential metabolites and evaluation of their activity by a non cellular assay using recombinant human enzyme. *J. Enzymol. Inhib. Med. Chem.* **2004**, *19*, 17−32.
(48) Wachall, B. G.; Hector, M.; Zhuang, Y.; Hartmann, R. W. Imidazole substituted biphenyls: a new class of highly potent and in vivo active inhibitors of P450 17 as potential therapeutics for treatment of prostate cancer. *Bioorg. Med. Chem*. **1999**, *7*, 1913−1924.
(49) Pelkonen, O.; Raunio, H.; Rautio, A.; Pasanen, M.; Matti A. L. The metabolism of coumarin. ref 37, Chapter 3.
(50) Seliger, B. The effects of coumarin and its metabolites on cell growth and development. ref 37, Chapter 4.
(51) Pelkonen, O.; Rautio, A.; Raunio, H.;; Pasanen, M. CYP2A6: a human coumarin 7-hydroxylase. *Toxicology* **2000**, *144*, 139−147 and references therein.
(52) Still, W. C.; Kahn, M.; Mitra, A. Rapid chromatographic technique for preparative separations with moderate resolution. *J. Org. Chem.* **1978**, *43*, 2923−2925.
(53) SYBYL 6.9.2 Tripos Inc., 1699 South Hanley Rd., St. Louis, MO 63144.
(54) McMartin, C.Bohacek, R. S. QXP: powerful, rapid computer algorithms for structure-based drug design. *J. Comput.-Aided Mol. Des*. **1997**, *11*, 333−344.
(55) GOLPE 4.5.12; Multivariate Infometric Analysis: Perugia, Italy, 2003.

JM049535J